Numerical simulation of risk mitigation methods for early age thermal cracking of concrete

2019

Presented at Concrete 2019 Conference, Sydney

Authors

Maryam Gharehchaei, Ph.D. Candidate, University of NSW

Ali Akbarnezhad, Associate Professor, The University of Sydney

Alireza Akbarzadeh Chiniforoush, Research Associate, The University of Sydney

Arnaud Castel, Associate Professor, University of NSW

Farzad Moghaddam, Senior Materials Engineer, Boral Innovation Factory Australia

Louise Keyte, General Manager, Boral Innovation Factory Australia

Luke Dingle, General Manager – Concrete Solutions and Business Improvement, Boral Australia

Stephen Foster, Professor, University of NSW

Numerical Simulation of Risk Mitigation Methods for Early Age Thermal Cracking of Concrete

Maryam Gharehchaei (Ph.D. Candidate, UNSW), Ali Akbarnezhad (Associate Professor, The University of Sydney), Alireza Akbarzadeh Chiniforoush (Research Associate, The University of Sydney), Arnaud Castel (Associate Professor, UNSW), Farzad Moghaddam (Senior Materials Engineer, Boral Innovation Factory), Louise Keyte (General Manager, Boral Innovation Factory), Luke Dingle (General Manager - Concrete Solutions and Business Improvement, Boral Australia) and Stephen Foster (Professor, UNSW)

Abstract

Minimising the risk of early age thermal cracking is a major challenge faced by the concrete industry when dealing with mass concrete, large restrained concrete elements, and concrete with high cement content. With this in mind, several numerical simulation models and guidelines have been developed to predict the temperature rise in concrete and to provide guidelines on design of reinforcements to limit the width of resulting cracks. However, such models have a number of key limitations which include inability to consider the effect of admixtures, providing 2D rather than 3D representation of the element, and inability to investigate different risk minimisation scenarios including placement of concrete in multiple layers, mix optimisation and embedment of cooling pipes. Among these, the latter is of particular importance as it considerably limits the ability of concrete specialists in dealing with high risk scenarios. In this paper, the working principles and features of a novel multi-physics numerical simulation model developed to address the above limitations is presented. The proposed model is then applied to three different real-life case studies to demonstrate its application in evaluating the effectiveness of sequential concrete placement and internal cooling strategies on minimising the risk of early age thermal cracking in the presented case studies.

Keywords: 3D numerical modelling, early age thermal cracking, sequential concrete placement, internal cooling system

1. Introduction

Early age thermal cracking due to hydration induced internal heating of concrete and subsequent cooling is one of the major issues affecting the structural performance and serviceability of concrete elements [1]. Numerical modelling of heat transfer in concrete by considering cement hydration as the heat source is commonly used to estimate the development of temperature and temperature gradient and consequently the risk of early age thermal cracking of concrete. Accordingly, several numerical simulation models have been proposed by previous studies to estimate the risk of early age thermal cracking of concrete [1–5]. However, the existing models have a number of important limitations including i) the1-D and 2-D nature of the analysis which limits the applicability of the model solely to cases that can be simplified to 1-D and 2-D; ii) the limited number of pre-defined geometries and the inability to add new customized element geometries; iii) inability to account for the effect of reinforcement on heat transfer; and iv) inability to accept direct calorimetry measurements as heat source which limits the precision of the model to the precision of the hydration heat estimates [1–5]. However, regardless of the modelling errors introduced by these limitations, the results of numerical simulation can be beneficial to evaluate the comparative risk of early age cracking associated with different concrete mixes. This provides a basis for optimizing the concrete mix design as an effective strategy to reduce the risk of early age thermal cracking of concrete [6].

However, when exposed to high risk of early age thermal cracking, concrete mix optimization alone may result in inadequate decrease in the risk level; and the use of supplementary strategies including sequential placement of concrete or internal cooling of concrete through embedded cooling pipes are commonly considered [7,8]. “Alternate bay” or “sequential” placement of concrete involves placing the concrete in multiple layers, with one or more days of delay between placement of each layer; and is a common strategy to reduce the risk of early age thermal cracking in massive concrete elements [9,10] Internal cooling, on the other hand, relies on pumping chilled water or air through a network of pipes embedded in concrete to absorb the heat of hydration of the materials and reduce the temperature rise in concrete [7,11] . However, sequential placement and internal cooling strategies are costly and usually introduce delays in completion of the concrete placement task; and therefore, are considered commonly to be the last resort. The costs and delays associated with sequential placement strategy is controlled directly by the duration of delay between casting of different layers and the number of layers, which is determined by chosen thickness for the layers. Identifying the required delay between placement of different layers and the thickness of each layer is a complex decision, affecting directly both the effectiveness of the strategy and its associated costs; and therefore, availability of decision support data to assist this decision is critical. Similarly, cost of internal cooling strategy and its effectiveness are controlled directly by the selected length and spacing of pipes in concrete; which should be optimized to minimize the costs while maximizing the effectives of the strategy. However, there is currently a lack of

reliable model to evaluate the effectiveness of selected implementation plan for sequential placement and internal cooling strategies at the planning stage, commonly leading to conservative planning and additional unnecessary costs.

This paper presents a comprehensive three-dimensional numerical simulation model aimed at estimating the risk of early age thermal cracking of concrete and the effectiveness of sequential placement and internal cooling strategies in reducing the risk. The proposed model addresses the limitation of the existing methods by allowing for a high level of customization in terms of geometry, materials properties, and inclusion of reinforcement. The proposed model is applied to three case studies to highlights its application in evaluating the effectiveness and optimizing sequential placement and internal cooling strategies.

2. Numerical simulation model

The proposed Multiphysics numerical simulation model performs heat transfer, solid mechanics, and coupled heat transfer-solid mechanic analyses by relying on relevant modules developed in COMSOL Multiphysics. Moreover, to integrate the time-dependent variable during the calculations, the model is coupled with time-dependent Ordinary Differential Equation (ODEs) interface.

To analyse the heat transfer in hardening concrete, defining the heat source and thermal boundaries is needed. The heat generation due to hydration of cement can lead to heat transfer inside and outside the concrete element [12–14]. The proposed model is designed to provide two alternative approaches for estimating the variations in the heat input to the model. These include i) estimating the heat generation using the Arrhenius equation [15], and ii) the direct use of isothermal calorimetry measurements for a particular mix. The second approach is recommended when using concrete mixes containing supplementary cementitious materials (SCMs) or retarders due to significant errors in prediction of heat generation using existing hydration heat models [16]. Given the time-consuming nature of calorimetry measurements, the proposed model is designed to accept calorimetry measurements in 5 or 10 °C interval, while using an interpolation function, Equation 1, to identify the hydration heat at other temperatures.

$$\mathrm{H(t)} = \frac{\mathrm{T}-\mathrm{T_1}}{\mathrm{T_2}-\mathrm{T_1}}(\mathrm{H_2}-\mathrm{H_1}) + \mathrm{H_1} \qquad \text{Equation 1}$$

where T, is the concrete temperature at each point of the element at each time step, $\mathrm{T_1}$ and $\mathrm{T_2}$ are curing temperatures of the first and second calorimetry experiments, respectively and $\mathrm{H_1}$and $\mathrm{H_2}$ are the heat of hydrations measured through two different calorimetry tests for each time step. Thermal properties of hardening concrete including Thermal conductivity, specific heat and coefficient of thermal expansion of concrete, which are calculated over time as functions of degree of hydration, are estimated using Equations 2 to 4, respectively [17–21].

$$k_C(\alpha) = k_{ult} \times (1.33 - 0.33\alpha) \qquad \text{Equation 2}$$

Where $\mathrm{k_C}$ is the thermal conductivity of the hardening concrete, α is the degree of hydration, and $\mathrm{k_{ult}}$ is the ultimate thermal conductivity of the hardened concrete.

$$\mathrm{C_c}(\alpha) = \mathrm{C_{ult}} \times (1.25 - 0.25\alpha) \qquad \text{Equation 3}$$

Where $\mathrm{C_c}$ is the specific heat of hardening concrete, α is the degree of, and $\mathrm{C_{ult}}$ is the ultimate specific heat of hardened concrete.

$$\mathrm{CTE_c} = \frac{\mathrm{CTE_{ca}V_{ca}+CTE_{fa}V_{fa}+CTE_pV_p}}{\mathrm{V_{ca}+V_{fa}+V_p}} \qquad \text{Equation 4}$$

Where $\mathrm{CTE_c}$, $\mathrm{CTE_{ca}}$, $\mathrm{CTE_{fa}}$, and $\mathrm{CTE_p}$ are the coefficient of thermal expansion of concrete mix, coarse aggregates, fine aggregates, and cement paste, respectively and $\mathrm{V_{ca}}$, $\mathrm{V_{fa}}$, and $\mathrm{V_p}$ are the volume of coarse aggregates, fine aggregates, and cement paste. Degree of hydration is the ratio of heat released to total heat available as below [21].

$$\alpha(\mathrm{t}) = \frac{\sum \mathrm{H(t)}}{\mathrm{H_T}} \qquad \text{Equation 5}$$

where α(t) is the degree of hydration at time t, ΣH(t) is the cumulative heat of hydration released at time t (J/m3) and H_T is the ultimate heat of hydration of concrete. Furthermore, in this study, Equation 6 is employed to simulate the convection coefficient due to forced and free convections [22].

$$\mathrm{h} = \mathrm{C} \times 0.2782 \times \left[\frac{1}{\mathrm{T_{avg}}+17.8}\right]^{0.181} \times |\mathrm{T_s}-\mathrm{T_a}|^{0.266} \times \sqrt{1+2.8566 \times \mathrm{w}} \qquad \text{Equation 6}$$

where $\mathrm{T_{avg}}$ is the average air film temperature; C is a heat flow constant which is equal to 10.15, 15.89, and 20.4 for bottom, vertical, and top surfaces, respectively; and w is the wind speed. Equation 6 is for relatively smooth surfaces. In order to consider the surface roughness, the convection coefficient h should be multiplied by a roughness multiplier R_f. Also, the solar radiation is considered using a linear relationship between cloud cover and solar radiation as shown in Equation 7.

$$\mathrm{EH} = (0.91 - (0.7 \times \mathrm{C})) \times \mathrm{ETOA} \qquad 1$$

where EH is the surface horizontal solar radiation; C is the cloud cover fraction; and ETOA is the extraterrestrial horizontal solar radiation [23].

Solid mechanics model is employed to predict the thermal stresses developed in concrete and therefore the early age thermal cracking potential of concrete elements. De Schutter [24] states that compressive stresses, in hardening concrete, are usually much smaller than compressive strength; and therefore a linear relationship will be accurate enough for use at early ages. To estimate the stress development and cracking potential in concrete, a reliable estimate of development of compressive strength, tensile strength, Young's modulus, and Poisson's ratio at early ages is required. The proposed numerical model relies on previously verified time dependent empirical models, presented in Equations 8-12, to estimate the development of these properties over time [25–27]. The development of compressive strength is calculated using Equation 8.

$$f_c(t_e) = f_{cult} \times \exp\left(-\left(\frac{\tau_s}{t_e}\right)^{\beta_s}\right) \quad \text{Equation 8}$$

Where f_c and f_{cult} are the compressive strength and the ultimate compressive strength of concrete; τ_s and β_s are fitting parameters considered which are considered to be 27.8 (hour) and 0.721, respectively, and t_e is the equivalent age maturity [27]. The tensile strength is calculated using the following equation.

$$f_t = l \times (f_c)^m \quad \text{Equation 9}$$

Where f_t is the tensile strength development and l and m are fitting parameters, which are considered to be 0.3 and 0.66, respectively [28].

$$E = k \times (f_c)^n \quad \text{Equation 10}$$

Where E is the elastic modulus development (MPa), f_c is the compressive strength development (MPa), and n and k are fitting parameters, which are considered to be equal to 0.5, and k is calculated using Equation 11.

$$k = 0.043 \times {w_c}^{1.5} \quad \text{Equation 11}$$

where w_c is the density of fresh concrete.

$$\upsilon(\alpha) = 0.18 \times \sin\left(\frac{\pi \times \alpha}{2}\right) + 0.5 \times \exp(-10\alpha) \quad \text{Equation 12}$$

where υ is the Poisson's ratio.

In the bottom boundary, where the concrete mass is in contact with the foundation, high degree of resistant in both normal and shear directions are present. Therefore, the bottom boundary condition is defined as a spring foundation and the spring constant is determined by considering the rigidity of foundation using Equation 13.

$$k = \begin{bmatrix} GT & 0 & 0 \\ 0 & GT & 0 \\ 0 & 0 & 2.1e^{10} \end{bmatrix} \quad \text{Equation 13}$$

where, k is the sprig constant per unit area, GT is the modulus of rigidity of hardening concrete and $2.1e^{10}$ is the modulus of rigidity for hardened.

To numerically simulate the thermal expansion in concrete and the resulting thermal stresses, the heat transfer and solid mechanics models are coupled, so that the temperature and displacement fields will be analysed simultaneously. The thermal expansion of concrete is calculated using the following equation:

$$\varepsilon_{th} = CTE_c \times \Delta T \quad \text{Equation 14}$$

where, ε_{th} is the thermal strain, ΔT is the change of temperature, and CTE_c is the coefficient of thermal expansion of hardening concrete.

2.1. Simulation of Sequential Concrete Placement Strategy

This section highlights only the major modifications in the above model to allow analysis of sequential placement strategy. The heat source is defined as a separate function for each layer and is defined as a function of concrete placement time for each layer rather than the overall time of the analysis. Therefore, the hydration heat generation of each layer starts after its placement time. To achieve this, the equivalent age of each layer which is used in the Arrhenius equation for estimating the heat of hydration is defined by Equation 15.

$$t_e(T_r) = \sum_n^t \exp\left(\frac{E}{R}\left(\frac{1}{273+T_r} - \frac{1}{273+T_c}\right)\right).\Delta t \quad \text{Equation 15}$$

where n is the time of the placement of the n^{th} layer. Similarly, the top boundary condition of each layer is defined as a function of time so that after placement of top layer the type of boundary condition changes from convention to conduction. Similar to the base model, the spring foundation boundary condition for the bottom surface of the first layer, which seats on the foundation or ground, is defined based on Equation 13. Whereas, for the subsequent layers, the bottom surface of the layer seats on the hardening concrete of the previous layer and therefore its spring constant is calculated by:

$$k = \begin{bmatrix} GT & 0 & 0 \\ 0 & GT & 0 \\ 0 & 0 & GT\ (previous\ layer) \end{bmatrix} \quad \text{Equation 16}$$

2.2. Numerical modelling of internal water cooling

The proposed model allows for selecting the type of pipe material along with the rate of water flow, which is introduced as a laminar flow. The Navier-Stokes equation is defined as below for laminar flows.

$$\begin{cases} \rho\left(\frac{\partial u}{\partial t} + u.\nabla u\right) = -\nabla p + \nabla.(\mu\left(\nabla u + (\nabla u)^T - \frac{2}{3}\mu(\nabla.u)I\right) + F \\ \rho\nabla.u = 0 \end{cases}$$ Equation 17

where u is the fluid velocity, p is the fluid pressure, ρ is the fluid density, μ is the fluid dynamic viscosity and F is the external forces applied to the fluid [29]. After defining the geometry and location of the pipes in the structure, the water temperature is provided as an input to the model. It is assumed that the heat transfer happens through conduction between the liquid flow, the pipe, and the concrete surrounding the pipe. The concrete element is generating heat due to hydration. The heat in the water is assumed as below [30]:

$$\rho_w c_w\left(\frac{\partial T_w}{\partial t} + u.\nabla T_w\right) = k_w \nabla^2 T_w$$ Equation 18

where T_w is the temperature of water in the pipe, ρ_w, c_w and k_w are the density, specific heat and conductivity of water, respectively.

3. Case study

In order to evaluate the performance of the proposed numerical model, three different cases are studied. Case study 1 is a $13.07(L) \times 2.1(H) \times 1.2(T)\ (m)$ concrete wall built in one of Boral Ltd. Quarries in Queensland, Australia which is used for validating the numerically predicted temperature. Case study 2 is a dam foundation in Queensland, Australia with the dimensions of $14.9(L) \times 18.5(W) \times 1(T)\ (m)$ that is used to demonstrate the simulation of sequential concrete placement. Case study 3 is a real-world concrete pile with the dimensions of 2.4 (D)×15(H) (m) which is to demonstrate the effect of embedded cooling pipes on risk of early age thermal cracking. The mix design of concrete used for different is presented in Table 1.

Table 1 Mix design of concrete used in different case studies

Material	Case 1 (Kg/m^3)	Case 2 (Kg/m^3),	Case 3 (Kg/m^3),
Portland Cement	260	200	290
Fly Ash	-	90	120
Slag	173	-	140
Water	199	188.5	170
W/CM	0.46	0.65	0.31
Coarse Aggregate	1329	1022	980
Fine Aggregate	401	830	700

In order to verify the results of our proposed numerical model using case 1, in-situ measurement of temperature at 15 points (Figure 1) were carried using SmartRock2 wireless temperature sensors. The concrete wall was modelled numerically using the proposed numerical model and the temperature, thermal stresses and resulting cracking ratios were numerically obtained. Crack ratio is defined as the ratio of developed tensile stress to tensile strength in the early age concrete mass [27,31]. In particular, the temperature predictions at the coordinates corresponding to the exact location of embedded temperature sensors were used to validate the model. Case 2 is numerically modelled to investigate the effectiveness of sequential placement strategy in reducing the risk of early age thermal cracking of concrete. In particular, this case study aims at assisting the designers in selecting the best time interval for sequential concreting. The thickness of each layer is prescribed to be one meter based other construction requirements. The initial concrete temperature is 20ºC, and the numerical model is run for three scenarios, assuming 1, 2 and 3 days delay between placing different layers, respectively. To investigate the influence of the embedded water pipes on the maximum temperature, water piping system is modelled in the concrete pile (case 3). As shown in Figure 2, two water pipes with the inner and outer diameters of 0.03m and 0.035m were modelled inside the pile, which has a diameter of 2.4m. The heat capacity and the thermal conductivity of the material considered for pipes are 420 [J/(kg*K)] and 50 [W/(m*K)], respectively. The placement temperature of concrete and water temperature are considered as 32 ℃ and 20 ℃, respectively. The same pile was also modelled without the piping system in order to compare the results.

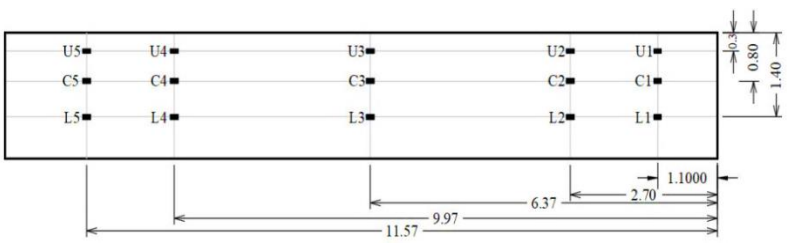

Figure 1 Embedded sensor locations (in meter)

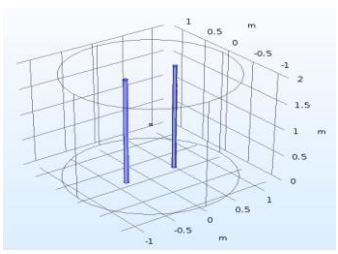

Figure 2 Embedded water pipes

4. Results and discussion

4.1. Case 1

Table 2 compares the measured and predicted maximum peak temperatures at all the points highlighted in Figure 1. Furthermore, Figures 3 and 4 show the variations in the temperature with time at two representative points inside the concrete element. As can be seen, the results confirm the acceptable precision of the numerical simulation model in predicting the temperature profile, which is a direct indicator for risk of early age thermal cracking of concrete. Therefore, the results suggest the reliability of the proposed model for numerical comparison of the relative risk of cracking associated with different mixes and different construction scenarios. Figures 6 and 7 illustrate the thermal stresses development in four selected points shown in Figure 5. Moreover, Figure 8 shows the crack ratio at the selected points. As can be seen, the crack ratio is the highest at Point D which is a corner point and the least crack ratio occurs in the middle point of the element.

Table 2. Case 1 - numerically predicted temepratures versus actual temperature measurements

Point	Max. measured temperature (DegC)	Max. Predicted Temperature (DegC)	Error (%)	Point	Max. measured temperature (DegC)	Max. Predicted Temperature (DegC)	Error (%)
U1	77.5	70.34	9.24%	L3	77.9	82.86	6.37%
L1	79.5	82.5	3.77%	U4	68.1	70.74	3.88%
U2	70.4	70.67	0.38%	C4	80.5	82.79	2.84%
C2	77.2	82.7	7.12%	L4	78.3	82.89	5.86%
L2	76.7	82.9	8.08%	U5	67.7	70.76	4.52%
U3	71.3	70.81	0.69%	L5	77.7	82.76	6.51%
C3	81	82.86	2.30%				

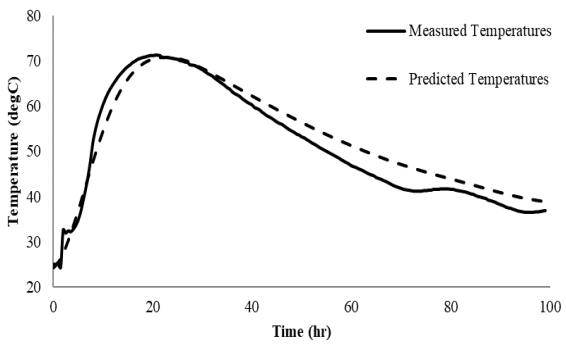

Figure 3 Comparison between numerical results and site measurements for point U3

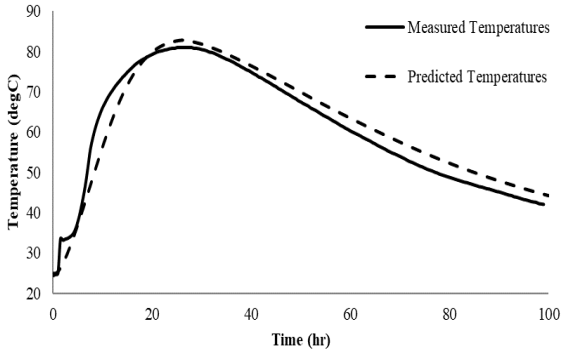

Figure 4 Comparison between numerical results and site measurements for point C3

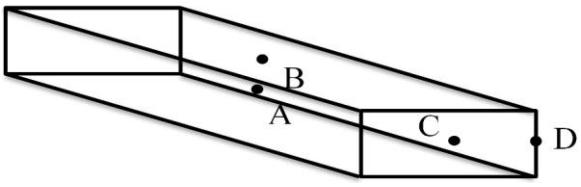

Figure 5 The studied points on the raft

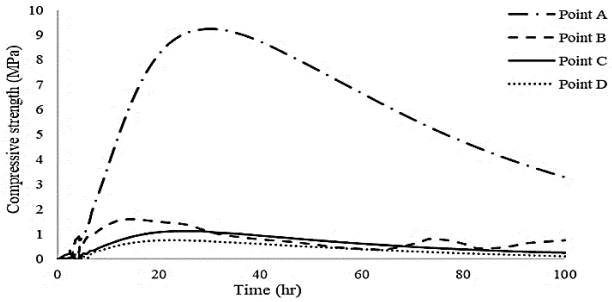

Figure 6 Thermal (compressive) stress development

4.2. Case 2

The heat development over time for a representative scenario (3 days delay between placement of different layers) at is shown in Figures 9 to 11, to illustrate the variations in the 3D destruction of temperature in the element over time. The predicted temperatures at 1 surface point as well as 15 points in the middle of different layers are shown in Figures 12 to 14. As can be seen, the temperature of point 1 at the end of the analysis is 29.0, 27.2 and 26.3 ℃ for the casting intervals of 1, 2 and 3 days, respectively. Furthermore, the slope of the cooling section of the curves for this point, which shows the rate of cooling, is -0.008, -0.013 and -0.017 for scenarios 1 to 3, respectively. This increase in the slope of

the cooling section is because an increase in placement intervals increases the duration of exposure of each first layer, thereby increasing the convection dominated cooling period.

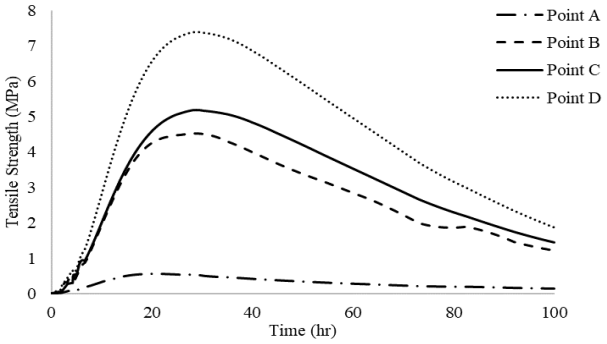

Figure 7 Thermal (tensile) stress development

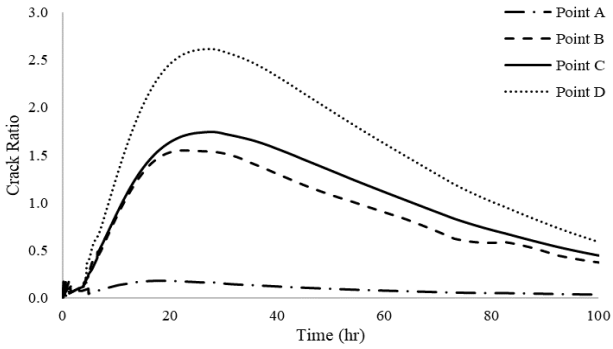

Figure 8 Crack ratio development

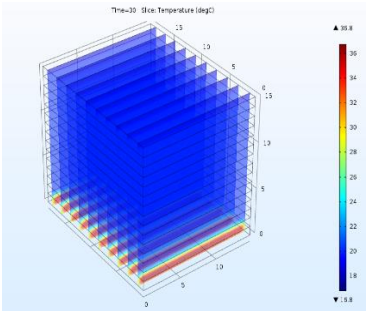

Figure 9 Heat transfer in the foundation at time= 30 hrs

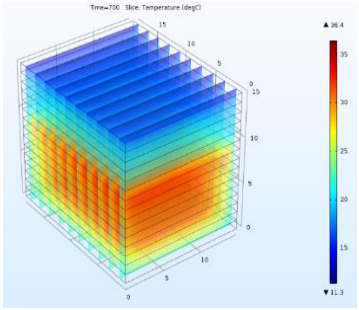

Figure 10 Heat transfer in the foundation at time= 700 hrs

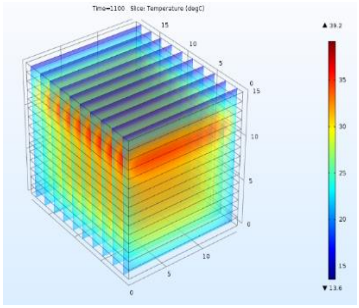

Figure 11 Heat transfer in the foundation at time= 1100 hrs

As shown, when placing the concrete every day, the middle layers seem to have little cooling opportunity and a distinct cooling phase is not apparent in the temperature profile. However, when the new layer is placed every 3 days, each layer could initiate the cooling phase. This in turn reduces the cumulative heat transmitted to the upper layers and consequently the maximum temperature. Therefore, as illustrated in Figure 15, the maximum temperatures within the concrete section is found to be 44.2, 42.4 and 39.0 °C for the concrete placement intervals of 1, 2 and 3 days, respectively. This indicates approximately 12% reduction in the maximum temperature of the foundation when increasing the sequential concrete placement interval from 1 to 3 days.

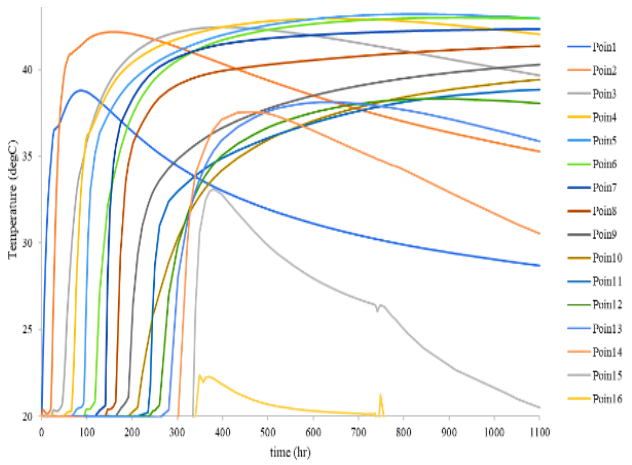

Figure 12 Temperature curves for different points of the foundation for the time interval of 1 day

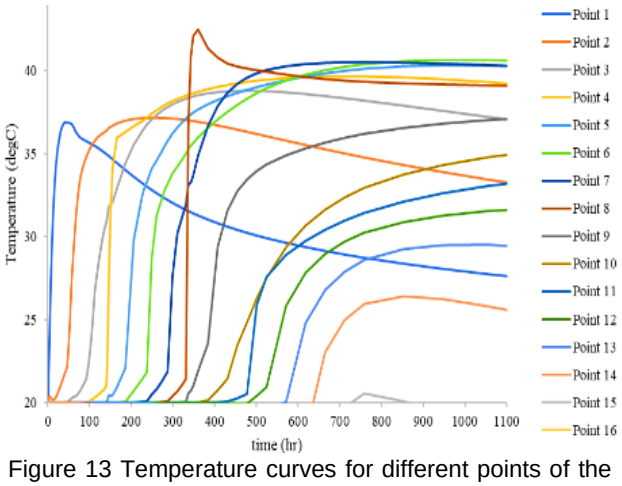

Figure 13 Temperature curves for different points of the foundation for the time interval of 2 days

Furthermore, the results show that the maximum temperature gradient between the middle point and the surface point of the foundation for three different concrete placement scenarios is respecitvely 3.3, 2.9 and 2.5 ($\frac{^{\circ}C}{m}$) for sequential concrete placement intervals of 1, 2 and 3 days. This indicates up to 25% decrease in the maximum temperature gradient, which is directly correlated to risk of early age thermal cracking, when the delay between placing different concrete layers increases from 1 day to 3 days. Similarly, the results indicate considerable decrease in the maximum crack ratio from 6.35 to 2.9 and 2.5 with an increase in delay between placement of different layers from 1 to 2 and 3 days, respectively.

Accordingly, the cracking risk is found to decrease by about 60% when increasing the concrete placement interval from 1 to 3 days.

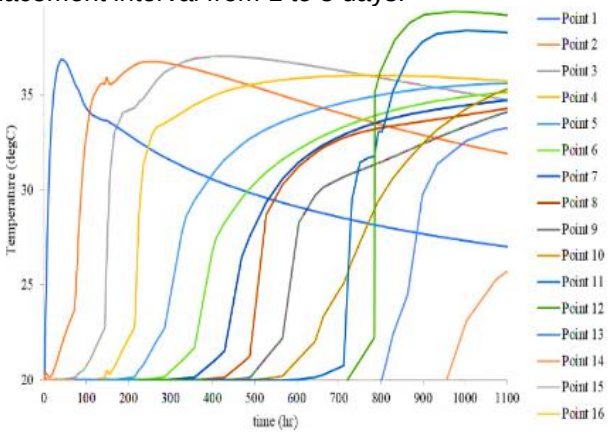

Figure 14 Temperature curves for different points of the foundation for the time interval of 3 days

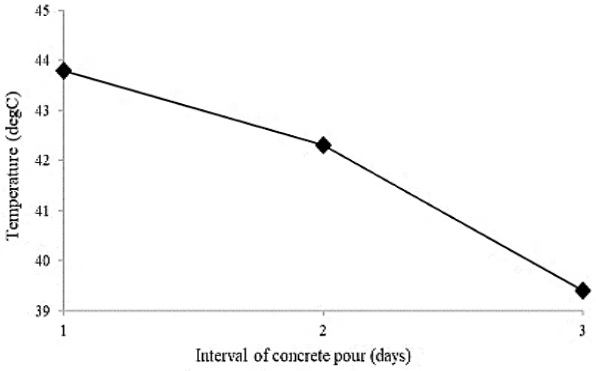

Figure 15 Maximum temperature within the foundation

4.3. Case 3

Temperature development within the concrete pile with embedded water piping system is shown in Figures 16 to 18 at different time steps during the analysis. As can be seen water pipes prevent the extreme temperature rise within the concrete pile. The effect of internal cooling on the maximum temperature of the middle point of the pile is presented in Figure 19. As can be seen, the use of internal cooling pipes results in a significant reduction in the maximum temperature of the pile from 103.9 ℃ to 79.4 ℃. Moreover, the maximum temperature gradient was reduced about 30% when using the cooling pipes which led to about 20% reduction in the maximum cracking ratio of the pile. This highlights internal cooling using embedded water pipes water piping system is an effective way to reduce the maximum temperature of the casted concrete element.

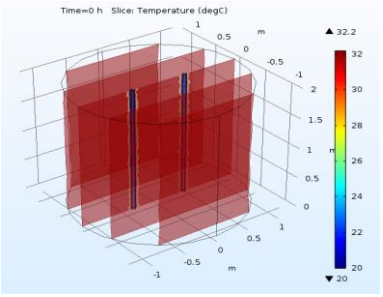

Figure 16 Temperature distribution of the pile with piping system at t=0 hours

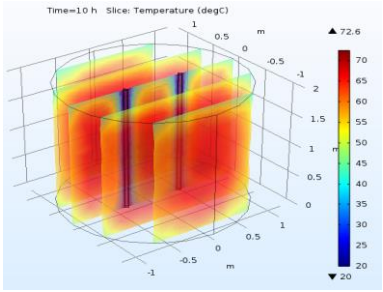

Figure 17 Temperature distribution of the pile with piping system at t=10 hours

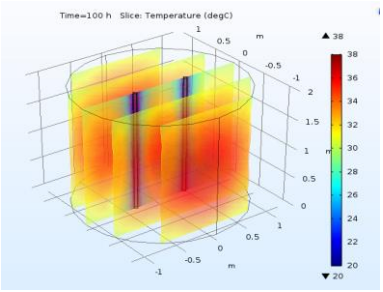

Figure 18 Temperature distribution of the pile with piping system at t=100 hours

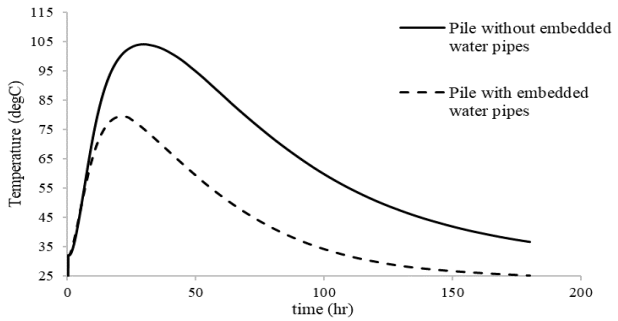

Figure 19 The effect of using embedded water pipes on maximum temperature in the pile

5. Conclusion

A comprehensive 3D numerical simulation model to predict the risk of early age thermal cracking of concrete was presented. The results of three case studies were used to demonstrate the precision of proposed 3-D numerical simulation model and its applications in i) predicting the temperature rise and risk of early age thermal cracking in concrete and ii) evaluating the efficiency of sequential concrete placement and internal cooling (using embedded pipes) strategies in mitigating the risk of early age thermal cracking. As demonstrated by case studies, the results of numerical simulation can provide concrete specialists and designers with unique decision support data to select an effective risk mitigation strategy to deal with concrete elements subject to high risk of early age thermal cracking. Furthermore, as

demonstrated by the results, through comparing the outcome of different scenarios, the proposed numerical makes available a unique tool to optimise key planning variables in the selected strategy, e.g. the optimal time interval between placing different layers in the sequential placement strategy.

Acknowledgement

The writers would like to acknowledge the support of Australian Research Council for this research support through ARC Linkage Grant LP150100725 as well as the funding and technical support provided by Boral Cement Australia**.**

References

[1] D. Ye, Early-age concrete temperature and moisture relative to curing effectiveness and projected effects on selected aspects of slab behavior, (2008). http://gradworks.umi.com/32/81/3281186.html.
[2] K. Folliard, M. Juenger, A. Schindler, J. Whigham, J. Meadows, FHWA/TX-08/0-4563-1 Prediction Model for Concrete Behavior., 7 (2008) 77.
[3] K.A. Riding, J.L. Poole, A.K. Schindler, M.C.G. Juenger, K.J. Folliard, Evaluation of temperature prediction methods for mass concrete members, ACI Mater. J. 103 (2006) 357–365.
[4] B. Kuriakose, B.N. Rao, G.R. Dodagoudar, V. Venkatachalapathy, Modelling of heat of hydration for thick concrete constructions - A note, J. Struct. Eng. 42 (2015) 348–357.
[5] M. Cervera, R. Faria, J. Oliver, T. Prato, Numerical modelling of concrete curing, regarding hydration and temperature phenomena, Reforma y Democr. 80 (2002) 1511–1521.
[6] M. Ghareh Chaei, A. Akbarnezhad, A. Castel, F. Moghaddam, S. Foster, A Genetic Algorithm Mix Optimization Model to Minimize the Risk of Early Age Thermal Cracking of Concrete, In Press, (2019).
[7] P. Groth, H. Hedlund, Air cooling of concrete by means of embedded cooling pipes—Part II: Application in design, Mater. Struct. 31 (2006) 387–392.
[8] P. Bamford, Early-Age thermal crack control in concrete, Constr. Ind. Res. Inf. Assoc. (2007) 23.
[9] H.G. Kwak, Y.J. Seo, C.M. Jung, Effects of the slab casting sequences and the drying shrinkage of concrete slabs on the short-term and long-term behavior of composite steel box girder bridges. Part 1, Eng. Struct. 22 (2000) 1453–1466.
[10] L. Dezi, F. Gara, G. Leoni, Construction sequence modelling of continuous steel-concrete composite bridge decks, Steel Compos. Struct. 6 (2006) 123–138.
[11] Y. Hong, W. Chen, J. Lin, J. Gong, H. Cheng, Thermal field in water pipe cooling concrete hydrostructures simulated with singular boundary method, Water Sci. Eng. 10 (2017) 107–114.
[12] F.P. Incropera, D.P. DeWitt, Introduction to heat transfer, Wiley, New York, 1985.
[13] L.T. Bergman, S.A. Lavine, P.F. Incropera, P.D. DeWitt, Fundamentals of Heat and Mass Transfer, John Wiley & Sons, Inc., New York, 2011.
[14] L. Theodore, Heat Transfer Applications for the Practicing Engineer, 2011..
[15] Z.P. Bazant, J.K. Kim, S.E. Jeon, Cohesive fracturing and stresses caused by hydration heat in massive concrete wall, J. Eng. Mech. 129 (2003) 21–30.
[16] M. Ghareh Chaei, R. Lloyd, L. Keyte, A. Akbarnezhad, S. Foster, Precision of cement hydration heat models in capturing the effects of SCMs and retarders, (2017) 1–15.
[17] K. Van Breugel, S. Lokhorst, Stress-based crack criterion as a basis for prevention of through-cracks in concrete structures at early ages, … RILEM Conf. …. (2003).
[18] A.K. Schindler, Effect of Temperature and Curing on the Early Hydration of cementitious materials, ACI Mater. J. 101 (2004) 72–81.
[19] H. Reinhardt, J. Blaauwendraad, J. Jongedijk, Temperature development in concrete structures taking account of state dependent properties, Int. Conf. Concr. Early Ages. (1982).
[20] J.H. Emanuel, J.L. Hulsey, NoPrediction of the Thermal Expansion Coefficient of Concrete., J. Am. Concr. Inst. 74 (1977) 149–155.
[21] A.K. Schindler, K.J. Folliard, K. Schindler, A. and Folliard, Heat of hydration models for cementitious materials, ACI Mater. J. 102 (2005) 24–33.
[22] Ashrae, ASHRAE Handbook, Atlanta, 1993.
[23] G.S. WOJCIK, Effects of Atmospheric and Construction Conditions on Concrete Equivalent Ages, Mater. J. 101 (2004) 374–384.
[24] G. De Schutter, Finite element simulation of thermal cracking in massive hardening concrete elements using degree of hydration based material laws, Comput. Struct. 80 (2002) 2035–2042.
[25] E. Martinelli, E.A.B. Koenders, A. Caggiano, A numerical recipe for modelling hydration and heat flow in hardening concrete, Cem. Concr. Compos. 40 (2013) 48–58.
[26] K. a. Riding, J.L. Poole, A.K. Schindler, M.C.G. Juenger, K.J. Folliard, Statistical Determination of Cracking Probability for Mass Concrete, ASCE J. Mater. Civ. Eng. 26 (2013) 04014058.
[27] K. a Riding, Early Age Concrete Thermal Stress Measurement and Modeling, PhD Diss. (2007).
[28] J.M. Raphael, Tensile strength of concrete, ACI Mater. J. 81 (1984) 158–165.
[29] H. Nguyen, T. Hoang, Numerical Simulation of Laminar Flow Through a Pipe using COMSOL Multiphysics, Int. J. Sci. Eng. Res. 8 (2017) 290–295. http://www.ijser.org.
[30] J. Charpin, T. Myers, A.D. Fitt, N. Fowkes, Y. Ballim, A.P. Patini, PIPED WATER COOLING OF CONCRETE DAMS, (n.d.) 69–85.
[31] Y. Tian, X. Jin, N. Jin, Thermal cracking analysis of concrete with cement hydration model and equivalent age method, Comput. Concr. 11 (2013) 271–289.